N_2 desorption in the isothermal decomposition of N_2O on Rh(110) at low temperatures

Kenji Imamura[1] and Tatsuo Matsushima[2,*]

[1]*Graduate School of Environmental Earth Science, Hokkaido University, Sapporo 060-0810 Japan*
[2]*Catalysis Research Center, Hokkaido University, Sapporo 001-0021 Japan*

Received 3 May 2004; accepted 9 July 2004

Transient N_2 desorption was analyzed in an angle-resolved form while a constant N_2O flux was introduced to clean Rh(110) or an oxygen-modified one. Even at 60 K, the decomposition proceeded and the product N_2 desorption collimated at either $65 \pm 3°$ or $30 \pm 1°$ off normal towards the [001] direction.

KEY WORDS: nitrous oxide; decomposition; rhodium; angle-resolved product desorption; single crystalline surfaces.

1. Introduction

Nitrous oxide N_2O decomposition on rhodium has attracted much attention in the catalytic removal of nitrogen oxides because this metal is one of the best catalysts for NO reduction and the main byproduct, N_2O, is harmful and has a remarkable greenhouse effect. However, the decomposition mechanism remains unclear [1]. This letter is the first to deliver the angular distributions of desorbing product N_2 in the isothermal N_2O(a) decomposition on Rh(110) at low temperatures. Even at 60 K, the decomposition proceeded and the product N_2 showed multi-directional desorption.

The NO reduction mechanism via the intermediate N_2O(a) has frequently been proposed on rhodium to explain the concomitant formation of N_2O and N_2 [2]. However, this mechanism has not been experimentally proved. Difficulties in the kinetic approach come from the fact that (i) the removal of surface nitrogen is not rate-limiting and (ii) the reactivity of N_2O is very high on clean Rh(110) and is subject to surface oxygen [3,4]. In fact, recent work with near-edge X-ray absorption fine structure (NEXFAS) indicates the partial dissociation of N_2O(a) on Rh(110) at around 60 K, although desorbing N_2 was not confirmed [5]. On the other hand, the angular and velocity distributions of desorbing products can provide information on product desorption processes even if these are not rate-limiting because the distributions do not involve the reaction rate [6]. In fact, a peculiar distribution of desorbing product N_2 is useful to examine the surface-nitrogen removal pathways [7–9].

In previous studies of angle-resolved temperature programed desorption (AR-TPD), we reported that the decomposition of N_2O on Rh(110) yielded four N_2 desorption peaks in the range of 105–165 K [3,4]. Except for one peak due to desorption from adsorbed N_2, the others yielded a sharp collimation at around either 30 or 70° off normal towards the [001] direction, depending on the annealing temperature after oxygen adsorption. Such complexity may partly be induced by TPD procedures. We have successfully examined the angular distribution of desorbing N_2 in the *isothermal* N_2O decomposition at low temperatures and confirmed that at least three kinds of reaction sites were operative below 160 K.

2. Experimental

Two UHV apparatuses were used. One had LEED and XPS facilities [10] and the other had three chambers for AR-desorption measurements [11]. The reaction chamber in the latter was equipped with an Ar^+ gun, a cryo-plate cooled below 40 K and a mass spectrometer for angle-integrated (AI) desorption analysis. The cryo-plate yielded a large pumping rate (about 9 $m^3\ s^{-1}$) that prevented the N_2 scattered on the reaction chamber wall from penetrating the analyzer [12]. The collimator had a slit on each end, and the analyzer had another mass spectrometer for AR-signals. A Rh(110) crystal was rotated to change the desorption angle (θ; polar angle) in the plane along the [001] direction, i.e., perpendicular to the surface atomic trough [9].

$^{15}N_2O$ was introduced through a gas doser. The subsequent heating yielded $^{15}N_2$ desorption in the surface temperature (T_S) range of 60–180 K. Hereafter, ^{15}N is represented as N in the text. The N_2O desorption was also noticeable below 140 K at high exposures. The N_2O coverage, Θ_{N_2O}, was defined as the sum of the

*To whom correspondence should be addressed.
Fax: +81-11-706-9120; E-mail: tatmatsu@cat.hokudai.ac.jp

1011-372X/04/0900–0197/0

AI-TPD peak areas of N_2 and N_2O relative to the value at the completed first layer. This completion was defined by the appearance of a sharp N_2O peak from the multilayer at 80 K in TPD procedures. The saturation level of N_2O(a) was less than half a monolayer from a comparison with the results on Pd(110) [13].

The LEED observations showed a strong (1×1) structure with a very weak (2×1) form after high N_2O exposures at 90 K. This structure was converted into intense (1×3) or (1×2) spots after heating above 400 K. These super-structures disappeared by heating at 1100 K for 6 min. The resultant surface was used as the oxygen-modified one because the subsequent N_2 desorption still involved the contribution from the oxygen-modified area. For the preparation of clean Rh(110), the surface was heated at 1200 K for 5 min. No carbon segregation was found during this heating by XPS after the crystal was cleaned once.

3. Results

3.1. Clean surface

A significant amount of N_2 emission was found even at $T_S = 60$ K when the clean surface was exposed to N_2O. The desorbing N_2 was analyzed in the AR-form during N_2O exposure at a fixed pressure of $P_{N_2O} = 7.5 \times 10^{-7}$ Pa. The desorption was only transiently noticed and its intensity was sensitive to the desorption angle. Typical traces of the AR N_2 signal are shown in figure 1(a–d). The N_2 signal initially jumped and decreased to the steady value, which was due to the fragmentation of N_2O in the analyzer because it was independent of the desorption angle and proportional to the N_2O pressure. The N_2O pressure was kept quite constant (figure 1(e)). The incident N_2O flux decreased with increasing the shift from the normal incidence because the angle between the incidence of N_2O

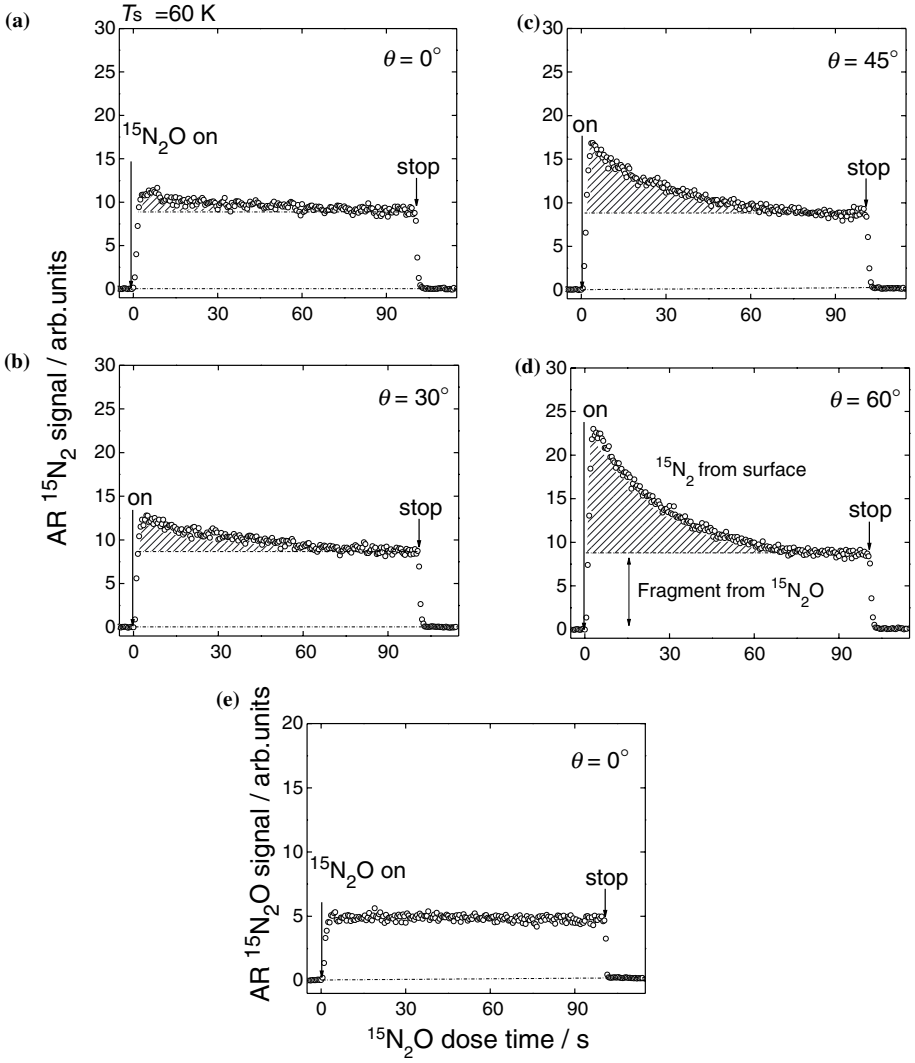

Figure 1. Isothermal $^{15}N_2O$ decomposition on clean Rh(110). (a-d)Variations of the AR-$^{15}N_2$ signal at different θ values with the $^{15}N_2O$ exposure time. $T_S = 60$ K, and $P_{N_2O} = 7.5 \times 10^{-7}$ Pa. The steady value of the $^{15}N_2$ signal is due to the fragmentation of $^{15}N_2O$. (e) AR-$^{15}N_2O$ signal at the normal direction.

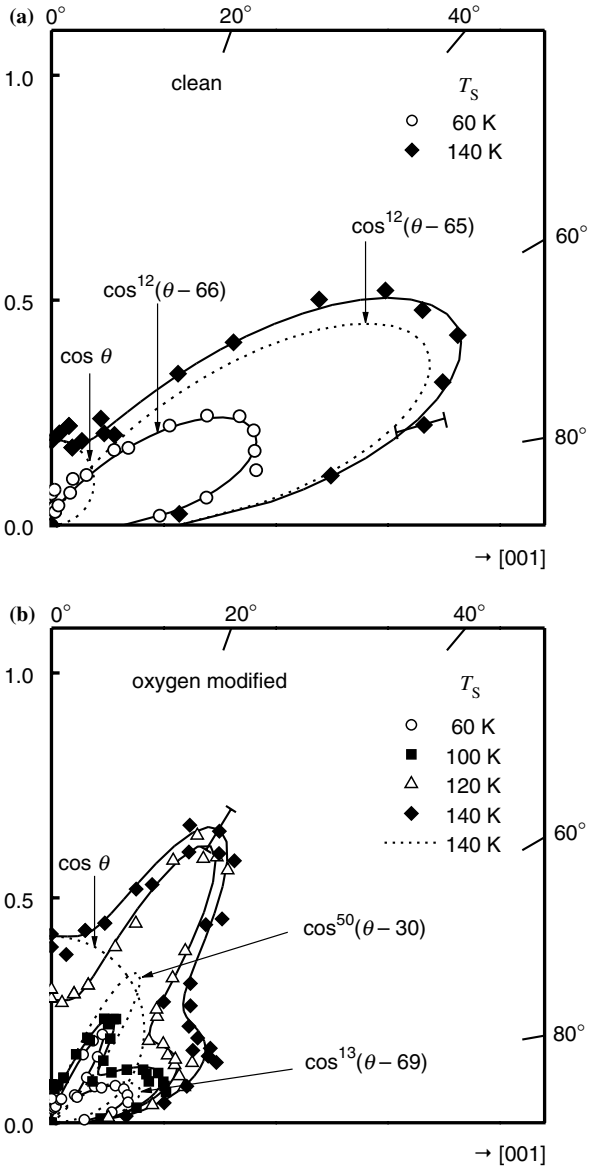

Figure 2. Angular distributions of desorbing $^{15}N_2$ in isothermal $^{15}N_2O$ decomposition in the plane along the [001] direction at different T_S values. (a) Clean and (b) oxygen-modified surfaces. $P_{N_2O} = 7.5 \times 10^{-7}$ Pa. Typical deconvolutions are shown by broken curves only for the data at $T_S = 140$ K to avoid confusions. The solid lines indicate the total signal of deconvoluted components.

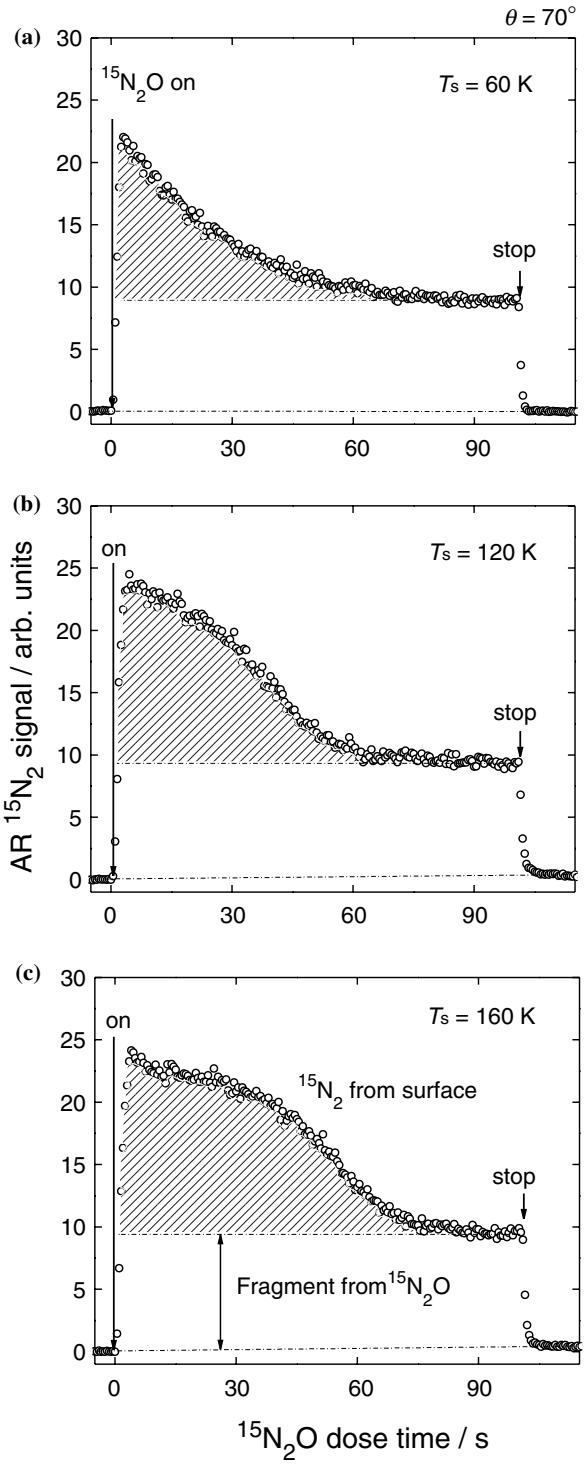

Figure 3. AR-$^{15}N_2$ signals at different T_S during the $^{15}N_2O$ exposure on clean Rh(110) at $\theta = 70°$ in the plane along the [001] direction. $P_{N_2O} = 7.5 \times 10^{-7}$ Pa.

exposure and the detection of desorbing N_2 was fixed at 45°. The amount of N_2 produced above the steady-state line (the crossed hatched area) is plotted against the desorption angle in figure 2(a). The N_2 signal was not normalized to the value for the N_2O flux at the normal incidence because the integrated amount rather than the N_2 signal increment was plotted. In fact, the duration of N_2 emission was somewhat extended at larger incident angles. The N_2 desorption sharply collimated at 66° off normal. The intensity was approximated as $\cos^{12}(\theta\text{-}66)$.

With increasing fixed T_S, the N_2 formation was enhanced as shown in figure 3. At $T_S = 60$ K, the N_2 formation decreased rapidly and monotonously. At 160 K, it was initially kept at a high value and decreased quickly. The produced N_2 amount estimated in the same way as above is plotted in figure 2(a). The formation at 140 K increased about twice that at 60 K, and the collimation angle remained almost invariant. The maximum N_2 signal at the beginning exposure increased

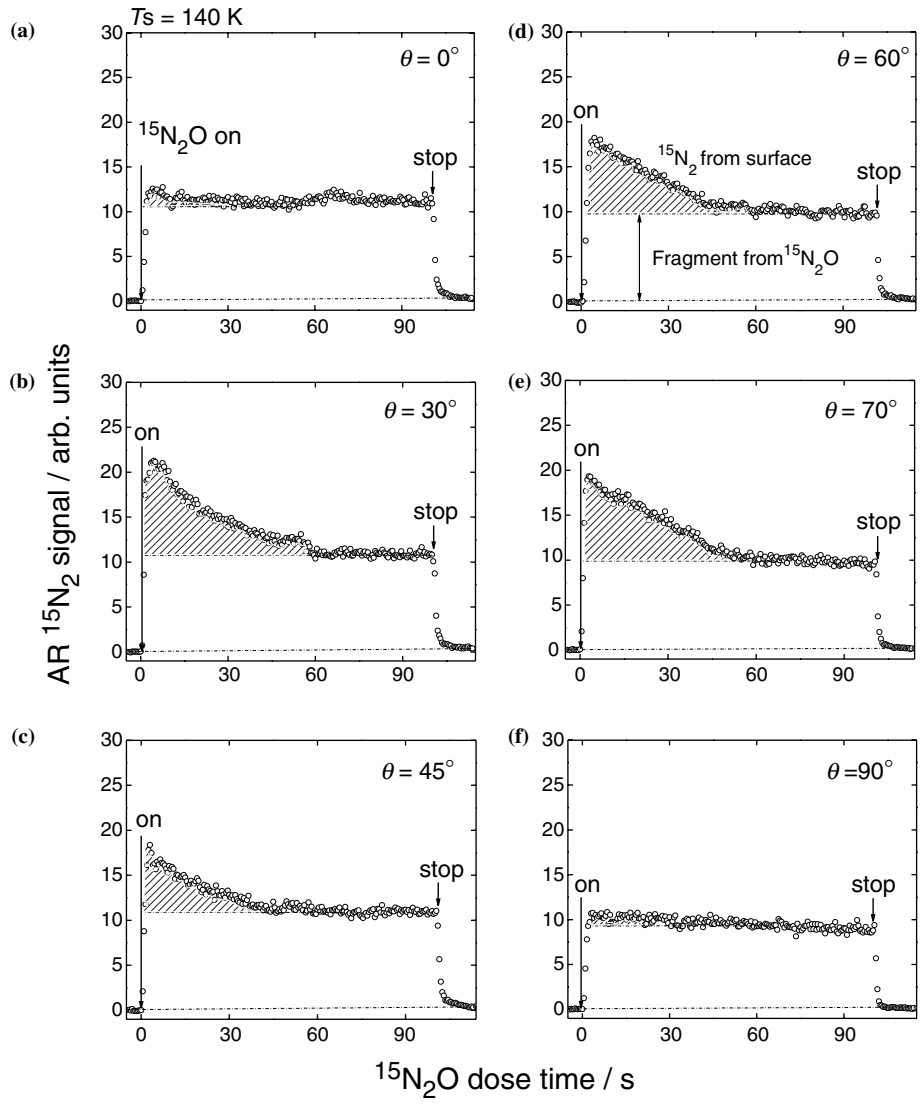

Figure 4. AR-$^{15}N_2$ signals during the $^{15}N_2O$ exposure on the oxygen-modified surface at different θ values in the plane along the [001] direction. T_S = 140 K, and $P_{N_2O} = 7.5 \times 10^{-7}$ Pa.

with increasing N_2O pressure, but the integrated amount above the fragment line remained invariant. The total N_2 formation at 60 K was estimated to be about 20% of that in post-TPD at saturation, where the surface was highly covered by N_2O, N_2 and oxygen atoms. This is because in the post-TPD, desorbing N_2 reached about 60% of the total desorption and N_2O shared about 40%. On the other hand, after N_2O exposure at 120 K or above it, the total desorption of N_2 and N_2O in the subsequent heating was less than a half of the amount of emitted N_2 during N_2O exposure. The amount of N_2O shared only about 25% or less.

3.2. Oxygen-modified surface

The angular distribution of desorbing N_2 on the oxygen-modified surface was very different from that on the clean surface. Here, a new desorption, collimated at around 30° off normal, also appeared. This desorption was sensitive to the surface temperature for annealing after N_2O or oxygen adsorption. Typical N_2 desorption traces at different θ values are shown in figure 4, where the surface was heated in advance at the flashing temperature T_{flash} = 1100 K for 6 min after N_2O exposure to saturation and then N_2O was dosed at T_S = 140 K. The remaining oxygen before N_2O exposure was estimated to be about 5% of the saturation in comparison with the N_2 formation after definite amounts of oxygen as described later. This oxygen was not on the surface because it was not removed by hydrogen exposure at around 400 K. The N_2 signal was high at around both 30 and 70°. The amount of N_2 formed above the fragment line is plotted on polar coordinates in figure 2(b). The desorption was collimated at around either 30 or 69°. The former component increased more than the other with increasing T_S for the

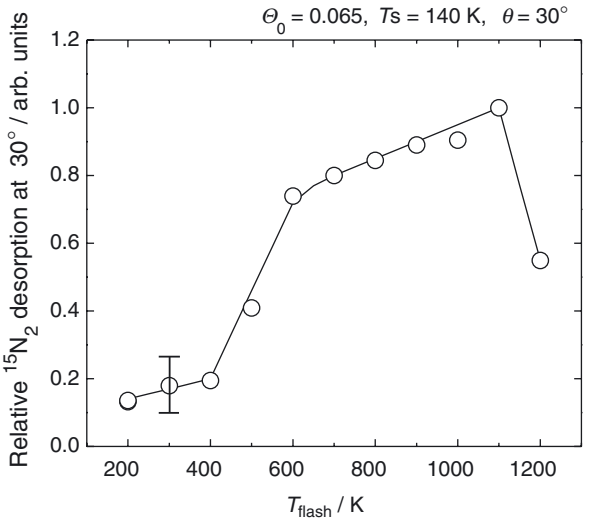

Figure 5. Surface annealing effect to the 30° component. The $^{15}N_2$ formation observed at $\theta = 30°$ in the plane along the [001] direction versus the surface flashing temperature (T_{flash}) after O_2 exposure and before $^{15}N_2O$ exposure. The O_2 exposure was only 6.5% of the saturation level. $P_{N_2O} = 7.5 \times 10^{-7}$ Pa.

N_2O exposure, suggesting that it was induced by the process with higher activation energy for N_2O dissociation. On the other hand, the 69° component was highly suppressed. A typical deconvolution is shown for the distribution at $T_S = 140$ K, where a cosine component was also enhanced [8].

The 30° component was enhanced with increasing T_{flash} value above 500 K. It was examined on modified surfaces that were flashed in advance to T_{flash} after 0.05 L (Langmuir; 1×10^{-6} Torr s ; 1 Torr = 133 Pa) O_2 exposure at $T_S = 300$ K. This oxygen exposure yielded a 0.065 monolayer without subsequent annealing. The transient N_2 formation at $T_S = 140$ K observed at 30° is plotted as a function of T_{flash} in figure 5. Without flashing, it was mostly suppressed, i.e., this small amount of oxygen was enough to prevent N_2O from decomposing. After flashing above $T_{flash} = 400$ K, the N_2 formation sharply increased at around 500 K. It increased slowly at $T_{flash} = 600$–1100 K and quickly decreased above it. This 30° component was completely suppressed after annealing at 1200 K for 5 min.

4. Discussion

4.1. Desorption components

N_2O is decomposed at 60 K, emitting N_2 in an inclined way. The total emission was only 20% of the desorbed N_2 in post-TPD at saturation. This amount increased with increasing surface temperature. Only two desorption components collimated at 30° and around 65°. The former was formed on the oxygen-modified site, probably in an oxide form, because it was completely suppressed on the clean surface and induced after heating above 500 K [2,14,15]. There are at least two kinds of oxygen atoms on the surface. One is the surface oxygen formed by O_2 exposure or N_2O dissociation below 400 K. The other is formed by annealing oxygen-covered surfaces above around 500 K. The former oxygen retards the N_2O dissociation at low temperatures and may shift the decomposition temperature upwards. This is caused by the stabilizing effect towards N_2O(a) [16] and the decreasing number of vacant sites. On the other hand, the oxide form provides the site for the 30° component.

Temperature-insensitive N_2 formation at the beginning of exposures in the range of 60–160 K indicates that N_2O decomposition is controlled by its adsorption. The decomposition on the clean area may be proportional to $\lambda_{N_2O}(1 - \alpha_{01}\Theta_O - \alpha_{02}\Theta_{N_2O})$ where λ_{N_2O} is the N_2O collision frequency, Θ_O is the coverage of oxygen released from N_2O dissociation, and α_{01} or α_{02} indicates a parameter representing the blocking by O(a) or N_2O(a). At 60 K, a model in which only the vacant site at $\Theta_O \gg \Theta_{N2O}$ can dissociate N_2O(a) yields $\alpha_{01} = 4$–5. However, at higher temperatures, some O(a)-affected sites must become active because the N_2 signal does not monotonously decrease above 120 K. The rate on such sites may follow a $k_1(1-\alpha_1\Theta_O)\Theta_O\Theta_{N_2O}$ form where k_1 or α_1 is a rate constant or another blocking parameter. The condition of $\Theta_O \gg \Theta_{N_2O}$ was actually accepted above 120 K. The sum of the above two quantities can well describe the total N_2 signal. However, the activation energy involved in k_1 was not estimated because of extremely small Θ_{N2O} values at 140–160 K. No dissociation is assumed to proceed on the O(a)-affected site with more oxygen. It is known that at temperatures above around 500 K, N_2O is decomposed even on highly oxygen-modified sites on rhodium [17]. The complexity of N_2O decomposition on rhodium may be caused by the presence of various active sites operative at different temperatures.

The 65° component was formed on the oxide-free site without O(a) or with O(a). At higher N_2O exposures, both sites became inactive because of the increasing site modification. These observations are reminiscent of the four N_2 desorption peaks in AR-TPD of N_2O(a) in the range of 105–165 K [3,4]. One of them, β_4-N_2, observed below 120 K in the TPD work, collimated at around 70°, whereas two others, β_2-N_2 and β_3-N_2, collimated at around 30°. The other, β_1-N_2, desorbed from N_2(a) because of the cosine distribution.

4.2. N_2 inclined desorption

A recent NEXAFS study showed that lying N_2O was oriented along the [001] direction on Pd(110) [18], on which a similarly inclined N_2 desorption was observed in the subsequent heating [13]. The latter form was supported on Pd(110)(1×1) by a density-functional theory calculation [19], where the lying form of N_2O is

in a bending configuration, bridging atomic Pd troughs extending in the [1$\bar{1}$0] direction. A similar N_2O admolecule may be on Rh(110)(1 × 1).

The direction of N_2 desorption is controlled by the balance between the repulsive forces from surface rhodium atoms and those from the nascent oxygen atom with high energy [9]. For the 65° component, the N_2O being dissociated must be in a form close to the surface parallel and oriented along the [001] direction because repulsions operating closely parallel to the surface plane are only possible from the nascent oxygen along the ruptured N–O bond. The presence of O(a) does not affect this collimation.

For the 30° component with a very sharp collimation, only the repulsive force from the nascent oxygen atom may be operative. No N_2O dissociation is expected on the reconstructed (1 × 2) part of Rh(110) because of the presence of a 0.5 monolayer of oxygen [2]. The remaining oxygen after annealing at 1100 K may be in an oxide form or located beneath the surface [14,15,20], where a highly inclined N_2O(a) interacting *with metal by the oxygen atom* is invoked. In fact, such inclined N_2O was predicted on positively charged Ag-clusters [21]. This kind of positive metal atom can be induced in oxides [22]. Thus, inclined N_2O may be formed on the site modified by oxygen in the oxide form. The N_2 collimation will be determined solely by the angle of the inclined N_2–O bond. This modified site is different from that in the above model to stabilize N_2O(a) by adsorbed surface oxygen. No information can be obtained for this oxide structure by LEED since only a sharp (1 × 1) pattern was observed. Probably, a low-temperature scanning tunneling microscope can identify the location of this site since it is attractive toward N_2O species.

5. Conclusions

Desorbing product N_2 was analyzed in the angle-resolved form when N_2O was dosed to Rh(110) at 60–160 K. The results are summarized as follows.

(1) Even at 60 K, the product N_2 desorption on the oxide-free site collimated at around 65° off normal towards the [001] direction. This desorption continued while O(a) accumulated although it retarded N_2O decomposition.
(2) The oxide site became active above 120 K and sharply emitted N_2 along 30° off normal toward the [001] direction.

Acknowledgments

This work was partly supported by Grant-in-Aid No. 13640493 for General Scientific Research from the Japan Society of the Promotion of Science. The authors thank Ms. Atsuko Hiratsuka for her drawings.

References

[1] F. Garin, Appl. Catal. A General 222 (2001) 183.
[2] G. Comelli, V.R. Dhanak, M. Kiskinova, K.C. Prince and R. Roseil, Surf. Sci. Rep. 32 (1998) 165.
[3] H. Horino, I. Rzeznicka, A. Kokalj, I. Kobal, Y. Ohno, A. Hiratsuka and T. Matsushima, J. Vac. Sci. Technol. A 20 (2002) 1592.
[4] S. Liu, H. Horino, A. Kokalj, I. Rzeznicka, K. Imamura, Y.-S. Ma, I. Kobal, Y. Ohno, A. Hiratsuka and T. Matsushima, J. Phys. Chem. B 108 (2004) 3828.
[5] H. Horino, I. Rzeznicka, T. Matsushima, K. Takahashi and E. Nakamura, in:*UVSOR Activity Report 2002* (Institute for Molecular Science, 2003) p. 211.
[6] I. Kobal, I. Rzeznicka and T. Matsushima in: Recent Research Developments in Physical Chemistry (Transworld Research Network) 6 (2002) 391 6 (2002) 391.
[7] I. Kobal, A. Kokalj, H. Horino, Y. Ohno and T. Matsushima, Trends Chem. Phys. 10 (2002) 139.
[8] T. Matsushima, Catal. Surv. Jpn. 5 (2002) 71.
[9] T. Matsushima, Surf. Sci. Rep. 52 (2003) 1.
[10] I.I. Rzeznicka, G. Moula, L. Morales de la Garza, Y. Ohno and T. Matsushima, J. Chem. Phys. 119 (2003) 9829.
[11] T. Matsushima, Surf. Sci. 127 (1983) 403.
[12] M. Kobayashi and Y. Tuzi, J. Vac. Sci. Technol. 16 (1979) 685.
[13] H. Horino, S. Liu, A. Hiratsuka, Y. Ohno and T. Matsushima, Chem. Phys. Lett. 341 (2001) 419.
[14] C. Africh, F. Esch, G. Comelli and R. Rosei, J. Chem. Phys. 115 (2001) 477.
[15] S. Suhonen, R. Polvinen, M. Valden, K. Kallinen and M. Härkönen, Appl. Surf. Sci. 200 (2002) 48.
[16] H.H. Huang, C.S. Seet, Z. Zou and G.Q. Xu, Surf. Sci. 356 (1996) 181.
[17] H. Uetsuka, K. Aoyagi, S. Tanaka, K. Yuzaki, S. Ito, S. Kameoka and K. Kunimori, Catal. Lett. 66 (2000) 87.
[18] H. Horino, I. Rzeznicka, T. Matsushima, K. Takahashi and E. Nakamura in: UVSOR Activity Report 2002 (Institute for Molecular Science, 2003) p. 209.
[19] A. Kokalj, I. Kobal and T. Matsushima, J. Phys. Chem. B 107 (2003) 2741.
[20] E. Schwarz, J. Lenz, H. Wohlgemuth and K. Christmann, Vacuum 41 (1990) 167.
[21] N.U. Zhanpeisov, G. Martra, W.S. Ju, M. Matsuoka, S. Coluccia and M. Anpo, J. Mol. Catal. A Chem. 201 (2003) 237.
[22] A.L. Yakovlev, G.M. Zhidomirov and R.A. Van Santen, Catal. Lett. 75 (2001) 45.